



HAL
open science

Effect of aluminium on the compressibility of silicate perovskite

Isabelle Daniel, Jay D. Bass, Guillaume Fiquet, Hervé Cardon, J. Z. Zhang, Michael Hanfland

► **To cite this version:**

Isabelle Daniel, Jay D. Bass, Guillaume Fiquet, Hervé Cardon, J. Z. Zhang, et al.. Effect of aluminium on the compressibility of silicate perovskite. *Geophysical Research Letters*, 2004, 31, pp.L15608. 10.1029/2004GL020213 . hal-00232722

HAL Id: hal-00232722

<https://hal.science/hal-00232722>

Submitted on 1 Feb 2021

HAL is a multi-disciplinary open access archive for the deposit and dissemination of scientific research documents, whether they are published or not. The documents may come from teaching and research institutions in France or abroad, or from public or private research centers.

L'archive ouverte pluridisciplinaire **HAL**, est destinée au dépôt et à la diffusion de documents scientifiques de niveau recherche, publiés ou non, émanant des établissements d'enseignement et de recherche français ou étrangers, des laboratoires publics ou privés.

Effect of aluminium on the compressibility of silicate perovskite

Isabelle Daniel,¹ Jay D. Bass,² Guillaume Fiquet,³ Hervé Cardon,¹ Jianzhong Zhang,⁴ and Michael Hanfland⁵

Received 9 April 2004; revised 15 June 2004; accepted 24 June 2004; published 5 August 2004.

[1] Volume measurements for aluminous MgSiO₃ perovskite containing 5 mol% Al₂O₃ were carried out up to pressures of 40 GPa at ambient temperature, using monochromatic synchrotron X-ray diffraction. A least-squares refinement of the data to the Birch-Murnaghan equation of state yields the following parameters $V_0 = 163.234(8) \text{ \AA}^3$, $K_{T0} = 251.5(13) \text{ GPa}$, $K'_0 = 4$. Within uncertainties, the presence of 5 mol% Al₂O₃ in MgSiO₃ perovskite induces a decrease of the bulk modulus in the range of 0% to 1.8%. Thus, K_T of perovskite is affected little if at all by the presence of Al³⁺. This result is in excellent agreement with the values deduced from sound velocity measurements on the same sample [Jackson *et al.*, 2004]. We discuss the possible origin of discrepancies among the different bulk moduli reported to date for aluminous perovskite. In light of recent calculations, our results are consistent with aluminium being dissolved in MgSiO₃ perovskite through a coupled substitution mechanism involving the replacement of both Mg²⁺ and Si⁴⁺ in the dodecahedral and octahedral sites by 2 Al³⁺. Moreover, any slight reduction in the bulk modulus of MgSiO₃ perovskite induced by the dissolution of 5 mol% Al₂O₃, indicates that the relative proportions of the minerals characteristic of the lower mantle, as inferred from seismological models, should not be significantly altered by the introduction of Al in the system. **INDEX TERMS:** 3620 Mineralogy and Petrology: Crystal chemistry; 3919 Mineral Physics: Equations of state; 3924 Mineral Physics: High-pressure behavior; 7205 Seismology: Continental crust (1242); 8124 Tectonophysics: Earth's interior—composition and state (1212). **Citation:** Daniel, I., J. D. Bass, G. Fiquet, H. Cardon, J. Zhang, and M. Hanfland (2004), Effect of aluminium on the compressibility of silicate perovskite, *Geophys. Res. Lett.*, 31, L15608, doi:10.1029/2004GL020213.

1. Introduction

[2] Deciphering the petrology of the Earth's lower mantle relies on knowledge of the individual thermoelastic properties of the minerals stable under the pressure and temperature conditions prevailing at such depths. MgSiO₃-perovskite (Mg-pv), as the end-member of the major phase in the lower mantle, has been the subject of numerous theoretical [e.g., Oganov *et al.*, 2001] and experimental studies [e.g., Fiquet

et al., 2000], which have recently converged upon a narrow range of values. From static compression experiments, the value of the isothermal bulk modulus K_0 is 253(9) GPa if the first pressure derivative K'_0 is fixed to 4, and 259 GPa with K'_0 adjusted to 3.7. Recent Brillouin scattering measurements yield a value for the adiabatic bulk modulus of $K_S = 253(3) \text{ GPa}$ [Sinogeikin *et al.*, 2004], in agreement with the lower values from compression experiments. Starting from the magnesian end-member, the effects of divalent cations (Ca²⁺, Fe²⁺) and trivalent cations (Al³⁺, Fe³⁺) on the thermoelastic properties of silicate perovskite have received comparatively little attention, considering that substitution of even large amounts of iron had not appeared to significantly change the bulk modulus of (Mg,Fe)SiO₃ perovskite.

[3] However, Zhang and Weidner [1999] found that the effect of Al on the compressibility of Mg-pv is dramatic. Perovskite with only 5 mol% Al₂O₃, which is commonly viewed as a typical concentration in the lower mantle, might have a bulk modulus 10% lower than the pure magnesian end-member. Such a large effect on K_T of Mg-pv, resulting from a minor amount of Al has been recognised at higher aluminium contents [Kubo *et al.*, 2000; Daniel *et al.*, 2001], whereas another recent experimental study showed that the bulk modulus of aluminous magnesium perovskite (hereafter referred to as Al-pv) is higher than that of Mg-pv [Andrault *et al.*, 2001]. Static first-principles Density Functional Theory (DFT) as well as atomistic calculations [Brodholt, 2000; Yamamoto *et al.*, 2003; Akber-Knutson and Bukowinski, 2004] have emphasized that dissolution of Al³⁺ into Mg-pv increases the compressibility of silicate perovskite. The extent to which K_0 decreases depends on the substitution mechanism of Al³⁺ into Mg-pv. The incorporation of Al³⁺ may occur by two competing mechanisms. The first is a coupled substitution $2 \text{ Al}^{3+} \rightarrow \text{Al}_{\text{Mg}} + \text{Al}_{\text{Si}}$ where Al enters both octahedral and dodecahedral cationic sites; it does not require the creation of vacancies for charge balance. In the second mechanism, Al replaces Si in the octahedral site only, and oxygen vacancies are thus created for charge balance. The calculated bulk moduli associated with the 'oxygen vacancy' mechanism are much lower than those related to the 'coupled substitution' mechanism, ~8% and ~2% lower than that of Mg-pv for 6.25 mol% Al₂O₃ incorporation, respectively [Yamamoto *et al.*, 2003]. Theoretical calculations also predict that the coupled substitution mechanism is energetically favoured, in agreement with Al EXAFS [Andrault *et al.*, 1998], ²⁷Al NMR measurements [Stebbins *et al.*, 2001], and thermodynamic measurements [Navrotsky *et al.*, 2003]. Hence, the few experiments carried out to date on the PV relationship of Al-pv have yielded highly contradictory results, which do not agree with the results of the DFT calculations. We have therefore performed a series of X ray diffraction measurements of Al_{0.5}-pv as a function of pressure, on a polycrystalline

¹Laboratoire de Sciences de la Terre, UMR 5570 CNRS-ENSL, Université Claude Bernard, Lyon, France.

²Department of Geology, University of Illinois, Urbana, Illinois, USA.

³Laboratoire de Minéralogie-Cristallographie UMR 7590, Université Paris VI, Paris, France.

⁴Los Alamos National Laboratory, Los Alamos, New Mexico, USA.

⁵European Synchrotron Radiation Facility, Grenoble, France.

sample containing 5 mol% Al_2O_3 . This sample was also investigated by Brillouin spectroscopy at ambient conditions [Jackson *et al.*, 2004], thus presenting a rare opportunity to determine the bulk modulus of exactly the same material by totally independent techniques.

2. Methods

2.1. Sample Description

[4] The $\text{Al}_{0.05}\text{-Pv}$ sample used in this X-ray diffraction study is from the same run charge as that employed in the Brillouin measurements by Jackson *et al.* [2004]. A single chip of material was cut into three parts, which were used in three different experiments. The sample was prepared from a synthetic glass composed of 80 mol% MgSiO_3 and 20 mol% $\text{Mg}_3\text{Al}_2\text{Si}_3\text{O}_{12}$ at ~ 25 GPa and 1873 K for two hours using a 2000-ton Kawai-type multi-anvil apparatus. A detailed characterization of the sample can be found in Jackson *et al.* [2004].

2.2. High-Pressure Techniques

[5] The samples were pressurized in membrane-type diamond anvil cells, mounted with 400 μm culet diamonds. We employed rhenium gaskets, indented to a thickness of about 80 μm , and drilled with 150 μm holes. After the sample was placed in the centre of the gasket hole, the sample chamber was filled with Ne at approximately 200 MPa, using a gas-loading device [Couzinet *et al.*, 2003]. Ne was chosen as a soft pressure medium, and also served as a pressure gauge. The pressure was measured before and after each x-ray exposure using the ruby fluorescence technique [Mao *et al.*, 1986]; pressure was also calculated from the equation of state of neon [Hemley *et al.*, 1989].

[6] At pressures higher than 26 GPa, the samples were systematically thermally annealed with a YAG laser at each pressure, for 5 at least minutes.

2.3. X-Ray Diffraction

[7] Angle dispersive diffraction measurements were carried out at the ID09 high-pressure beamline of the ESRF (Grenoble, France). The incident monochromatic X-ray beam at 0.4169 \AA was focussed and filtered through a

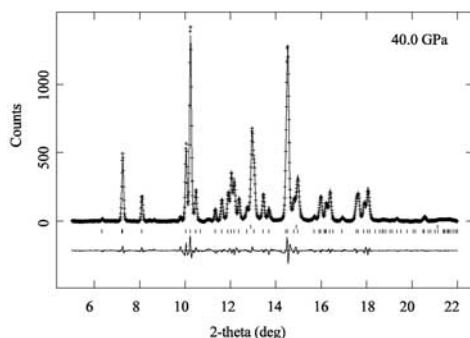


Figure 1. Representative X ray diffraction pattern of $\text{Al}_{0.05}$ -perovskite. Exposure time 10s at wavelength $\lambda = 0.4169$ \AA . The difference between calculated and observed intensities is shown at bottom and corresponds to a Le Bail refinement. Two series of ticks corresponding to the reflection lines of perovskite (bottom) and neon (top) are represented. See color version of this figure in the HTML.

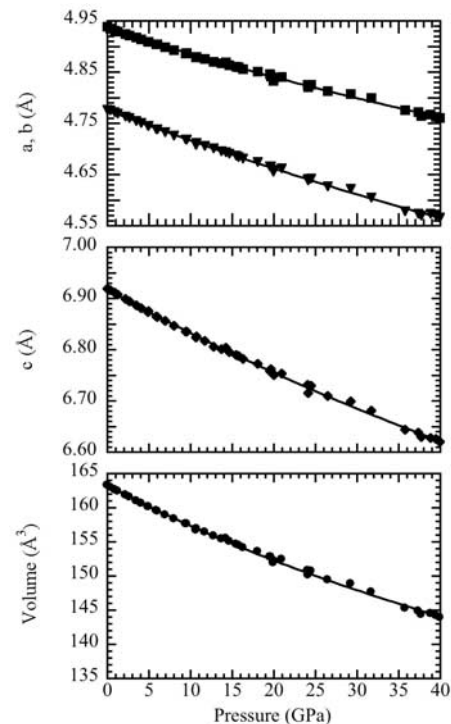


Figure 2. Variation of the unit-cell parameters and volume of $\text{Al}_{0.05}\text{-pv}$ with pressure at room temperature. The size of the data points greatly exceeds the experimental uncertainties. The lines are the equation of state fitted to the data.

60 μm pinhole to achieve a $30 \times 30 \mu\text{m}^2$ spot on the sample. The sample-detector (MAR CCD 345) was calibrated against a silicon standard prior to measurements. The diffracted signal was collected for 8 to 15 s, over a 2θ interval from 4 to 25 degrees. The two dimensional images were integrated after spatial distortion corrections using Fit2D [Hammersley *et al.*, 1996]. The 2θ patterns were processed using the GSAS package [Larson and Von Dreele, 1994]. Le Bail profile refinements were applied to a minimum of 60 diffraction lines, in order to obtain the unit cell parameters as a function of pressure (Figure 1).

3. Results and Discussion

3.1. Equation of State

[8] As shown in Figure 2, the volume and unit cell parameters of $\text{Al}_{0.05}\text{-pv}$ decrease smoothly with increasing pressure¹. A least-squares fit of the data using a weighting scheme, yields room pressure parameters $V_0 = 163.23(1) \text{\AA}^3$, $K_{70} = 251.5(13)$ GPa for the 2nd order Birch-Murnaghan equation of state, and $V_0 = 163.23(1) \text{\AA}^3$, $K_{70} = 251.5(27)$ GPa, $K'_{70} = 4.0(3)$ using a 3rd order Birch-Murnaghan equation. These results, as well as an f-F interpretation of the data, show that there is no significant departure of K'_{0T} from 4.

[9] Although the unit cell volume could not be measured at ambient condition, the values of $V_0 \text{\AA}^3$ from our regressions agree well with the value of 163.26(1) reported by

¹Auxiliary material is available at <ftp://ftp.agu.org/apend/gl/2004GL020213>.

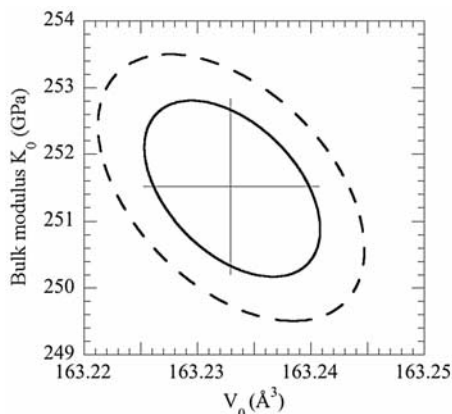


Figure 3. Confidence ellipses in K_0 and V_0 for the fit of the 2nd order Birch-Murnaghan EoS to the $\text{Al}_{0.05}\text{-pv}$ data (Table 1). The dashed and solid lines represent the limits calculated with 1σ error for 1 and 2 degrees of freedom, respectively. The 1σ error bars obtained from the variances of K_0 and V_0 are also reported.

Jackson et al. [2004] for the same sample. Our refined V_0 is also in good agreement with those measured or interpolated for similar compositions. Moreover, for the low compressions attained in the present data set, the refined ambient volume does not induce any systematic curvature on an f - F plot, which would be expected if V_0 were incorrect [Angel, 2000].

[10] In Figure 3 we show the $V_0 - K_{T0}$ confidence ellipse for the 2nd order Birch-Murnaghan equation-of-state fit to our data. The correlation coefficient between the two parameters is relatively high, with a value of -0.45 . This strong negative correlation between V_0 and K_{T0} should be considered in any further comparison of K_{T0} between silicate perovskite with different alumina content.

[11] The isothermal bulk modulus K_{T0} can be compared to the adiabatic bulk modulus K_{S0} calculated from the compression and shear velocities measured on the same sample [Jackson et al., 2004]. From the relation $K_s = K_{T0} (1 + \alpha\gamma T)$, using α the thermal expansion from Fiquet et al. [2000] and γ the Grüneisen parameter from Jackson [1998], we obtain for K_s a value of $253.6(13)$ GPa which is indistinguishable from $K_s = 252(5)$ reported by Jackson et al. [2004].

3.2. Comparison With the Existing Values of K_{T0}

[12] Compared with the average of reported values for Mg-pv, we find that the bulk modulus of $\text{Al}_{0.05}\text{-pv}$ is decreased by only 1.8% at most for an alumina content of 5 mol%. In fact, comparing our results with the bulk moduli of $K_{T0} = 253(9)$ by Fiquet et al. [2000] and $K_{S0} = 253(3)$ by Sinogeikin et al. [2004], there is no resolvable effect of Al on the bulk modulus of Al-pv within the experimental uncertainties. Hence, we find a much smaller effect of Al on the compressibility of perovskite than previous claims of about 10% for the same composition [Zhang and Weidner, 1999], or for higher Al content [Kubo et al., 2000; Daniel et al., 2001]. Our measurements do not support any increase of K_{T0} with Al substitution, as reported by Andraut et al. [2001].

[13] With the present experiments, we have attempted to determine as accurately as possible the subtle dependence

of the elastic properties of silicate perovskite on the Al content, even at low substitution levels. The capabilities of synchrotron radiation allow unit-cell parameters to be measured with a precision of 10^{-5} ; the critical factors for constraining K_{T0} therefore become the accuracy of the pressure scale and the presence of deviatoric stresses in the sample chamber. In the present experiment, two different pressure sensors were available: namely, ruby [Mao et al., 1986] and neon [Hemley et al., 1989]. Up to 25 GPa we used the ruby pressure scale, and obtained pressures equal to those deduced from the equation of state of neon within a $\pm 2\%$ difference. However the pressures determined by the two sensors showed systematic differences at higher pressures, when samples were annealed. Heated by conduction at the surface of the perovskite sample, neon recrystallises and stresses are released; stresses in neon near ruby, however, still build up with compression. As a consequence, pressure measured from ruby fluorescence was up to 5% higher than that given by neon, in the present experiment. This of course has considerable effects on the inferred compressibility of perovskite. For example, use of the ruby pressure scale throughout the experimental pressure range would have led to a K_{T0} value as high as $259(4)$ GPa, slightly higher than for Mg-pv and hence drastically changing our conclusions. This observation might explain the difference between the present results and those obtained by Andraut et al. [2001], in a study where pressures were also derived according to the ruby pressure scale.

[14] The large difference in K_{T0} between the present result and the low value obtained by Zhang and Weidner [1999] cannot be ascribed to the samples, which were both synthesized in a multi-anvil apparatus following the same procedure. However, the low K_{T0} value obtained by the latter might be due to the high-temperature (473–1073 K) but relatively low pressure (1.17–10.15 GPa) conditions at which in situ diffraction measurements were performed. For experiments performed out of the stability field of minerals, an underestimation of K_{T0} had been reported for several minerals, due to a high density of defects, to partial back-transformation, or even to partial amorphization at high temperature [Wang and Weidner, 1994]. Alternatively, the difference could also partly arise from the systematic errors in the Decker equation of state of NaCl used for determining pressure in the latter study.

[15] Compared to the low values of K_{T0} reported at higher aluminium content [Kubo et al., 2000; Daniel et al., 2001], the present result indicates the relationship between the bulk modulus of perovskite and the Al content is not a linear decrease, as previously suggested [Daniel et al., 2001]. There is a gap of approximately 10% between the bulk moduli of $\text{Al}_{0.05}\text{-}$ and $\text{Al}_{0.077}\text{-pv}$, which might be interpreted as a change in the dissolution mechanism of Al into perovskite with increasing the Al content in perovskite.

3.3. Substitution Mechanism of Al Into Perovskite

[16] Following the results of the most recent theoretical calculations for an Al-pv with a similar composition [Brodholt, 2000; Yamamoto et al., 2003; Akber-Knutson and Bukowinski, 2004], the 1.8% reduction in K_{T0} from the present results supports the energetically favoured coupled substitution mechanism, in the case of a perovskite

containing 5 mol% Al_2O_3 . Hence, numerical and experimental results suggest that coupled substitution is the dissolution mechanism effective at low Al content, up to 6.25 mol% Al_2O_3 at least [Yamamoto *et al.*, 2003]. However, the much lower value of K_{70} associated with perovskite with 7.7 mol% Al_2O_3 [Daniel *et al.*, 2001] suggests that the coupled substitution might evolve rapidly as the Al content in perovskite increases. That is, the oxygen vacancy mechanism may dominate over the coupled substitution mechanism in Al-rich perovskites. This would be consistent with the DFT calculations of Brodholt [2000], who showed that within the experimentally investigated pressure range, oxygen vacancies are energetically favoured for a perovskite structure with a high Al content, and that vacancy-bearing perovskites do have significantly greater compressibilities than those without such vacancies [Brodholt, 2000; Ross *et al.*, 2002].

3.4. Geophysical Inferences

[17] Results from the present study indicate that $\text{MgSiO}_3\text{-pv}$ with 5 mol% Al_2O_3 is not significantly more compressible than the magnesium end member. Considering that at lower mantle conditions Al dissolves almost entirely into $(\text{Mg, Fe})\text{SiO}_3\text{-pv}$ for peridotitic compositions, this would lead to a lower mantle petrology dominated by a silicate perovskite of composition $(\text{Mg, Fe, Al})(\text{Si, Al})\text{O}_3$, with minor amounts of magnesiowüstite and $\text{CaSiO}_3\text{-pv}$. Therefore, we discuss below the qualitative changes induced by the introduction of aluminium on models of the lower mantle which are often considered to be Al-free, and mainly based on optimizing linear combinations of the bulk moduli of relevant minerals to the K profile of whole-Earth models such as PREM. The present results show that the bulk modulus of $(\text{Mg, Al})\text{SiO}_3\text{-pv}$ is close to that of Mg-pv , thus not significantly changing previous models. However, the composition of magnesiowüstite is changed, since Fe partitions almost equally between perovskite and magnesiowüstite for Al contents similar to those above mentioned [Wood, 2000; Frost and Langenhorst, 2002]. Magnesiowüstite would therefore have an $\text{Fe}/(\text{Fe} + \text{Mg})$ ratio of approximately 0.1, and its bulk modulus would be similar to the MgO end member because the dependence of thermoelastic parameters of $(\text{Mg, Fe})\text{O}$ with iron substitution is very small [Zhang and Kostak, 2002]. As a result, the influence of aluminium on chemical and petrological models of the Earth's lower mantle, as deduced from seismic properties, is probably somewhat limited unless the coexistence of Al and Fe in Mg-pv results in combined effects that are as yet unknown.

[18] **Acknowledgments.** We are grateful to Jean-Claude Chervin for loading the cells with neon, and to J. M. Jackson and two anonymous reviewers for constructive comments. This research was supported by the NSF through grants EAR0003383 and 0135642, to JDB.

References

Akber-Knutson, S., and M. S. T. Bukowski (2004), The energetics of aluminum solubility into MgSiO_3 perovskite at lower mantle conditions, *Earth Planet. Sci. Lett.*, **220**, 317–330.
 Andraut, D., D. R. Neuville, A.-M. Flank, and Y. Wang (1998), Cation sites in Al-rich MgSiO_3 perovskites, *Am. Mineral.*, **83**, 1045–1053.
 Andraut, D., N. Bolfan-Casanova, and N. Guignot (2001), Equation of state of lower mantle (Al, Fe)- MgSiO_3 perovskite, *Earth Planet. Sci. Lett.*, **193**, 501–508.

Angel, R. J. (2000), High-pressure structural phase transitions, in *Transformation Processes in Minerals*, pp. 85–104, Mineral. Soc. of Am., Washington, D. C.
 Brodholt, J. P. (2000), Pressure-induced changes in the compression mechanism of aluminous perovskite in the Earth's mantle, *Nature*, **407**, 620–622.
 Couzinet, B., N. Dahan, G. Hamel, and J.-C. Chervin (2003), Optically monitored high-pressure gas loading apparatus for diamond anvil cells, *High Pressure Res.*, **23**, 409–415.
 Daniel, I., H. Cardon, G. Fiquet *et al.* (2001), Equation of state of Al-bearing perovskite to lower mantle pressure conditions, *Geophys. Res. Lett.*, **28**, 3789–3792.
 Fiquet, G., A. Dewaele, D. Andraut *et al.* (2000), Thermoelastic properties and crystal structure of MgSiO_3 perovskite at lower mantle pressure and temperature conditions, *Geophys. Res. Lett.*, **27**, 21–24.
 Frost, D. J., and F. Langenhorst (2002), The effect of Al_2O_3 on Fe-Mg partitioning between magnesiowüstite and magnesium silicate perovskite, *Earth Planet. Sci. Lett.*, **199**, 227–241.
 Hammersley, A. P., S. O. Svensson, M. Hanfland *et al.* (1996), Two-dimensional detector software: From real detector to idealised image or two-theta scan, *High Pressure Res.*, **14**, 235–248.
 Hemley, R. J., C. S. Zha, A. P. Jephcoat *et al.* (1989), X-ray diffraction and equation of state of solid neon to 110 GPa, *Phys. Rev. B*, **39**, 1820–1827.
 Jackson, I. (1998), Elasticity, composition and temperature of the Earth's lower mantle: A reappraisal, *Geophys. J. Int.*, **134**, 291–311.
 Jackson, J. M., J. Zhang, and J. D. Bass (2004), Sound velocities and elasticity of aluminous MgSiO_3 perovskite: Implications for aluminum heterogeneity in Earth's lower mantle, *Geophys. Res. Lett.*, **31**, L10614, doi:10.1029/2004GL019918.
 Kubo, A., T. Yagi, S. Ono, and M. Akaogi (2000), Compressibility of $\text{Mg}_{0.9}\text{Al}_{0.2}\text{Si}_{0.9}\text{O}_3$ perovskite, *Proc. Jpn. Acad.*, **76**, 103–107.
 Larson, A. C., and R. B. Von Dreele (1994), General structure analysis system, in *Los Alamos Manual*, report, pp. 86–748, Los Alamos Natl. Lab., Los Alamos, N. M.
 Mao, H. K., J. Xu, and P. M. Bell (1986), Calibration of the ruby pressure gauge to 800 kbar under quasi-hydrostatic conditions, *J. Geophys. Res.*, **91**, 4763–4767.
 Navrotsky, A., M. Schoenitz, H. Kojitani *et al.* (2003), Aluminum in magnesium silicate perovskite: Formation, structure, and energetics of magnesium-rich defect solid solutions, *J. Geophys. Res.*, **108**(B7), 2330, doi:10.1029/2002JB002055.
 Oganov, A. R., J. P. Brodholt, and G. D. Price (2001), Ab initio elasticity and thermal equation of state of MgSiO_3 perovskite, *Earth Planet. Sci. Lett.*, **184**, 555–560.
 Ross, N. L., R. J. Angel, and F. Seifert (2002), Compressibility of brownmillerite (CaFe_2O_7): Effects of vacancies on the elastic properties of perovskites, *Phys. Earth Planet. Inter.*, **129**, 145–151.
 Sinogeikin, S. V., J. Zhang, and J. D. Bass (2004), Elasticity of single crystal and polycrystalline MgSiO_3 perovskite by Brillouin spectroscopy, *Geophys. Res. Lett.*, **31**, L06620, doi:10.1029/2004GL019559.
 Stebbins, J. F., S. Kroeker, and D. Andraut (2001), The mechanism of solution of aluminum oxide in MgSiO_3 perovskite, *Geophys. Res. Lett.*, **28**, 615–618.
 Wang, Y. B., and D. J. Weidner (1994), Thermoelasticity of CaSiO_3 perovskite and implications for the lower mantle, *Geophys. Res. Lett.*, **21**, 895–898.
 Wood, B. J. (2000), Phase transformations and partitioning relations in peridotite under lower mantle conditions, *Earth Planet. Sci. Lett.*, **174**, 341–354.
 Yamamoto, T., D. A. Yuen, and T. Ebisuzaki (2003), Substitution mechanism of Al ions in MgSiO_3 perovskite under high pressure conditions from first-principles calculations, *Earth Planet. Sci. Lett.*, **206**, 617–625.
 Zhang, J., and P. Kostak (2002), Thermal equation of state of magnesiowüstite ($\text{Mg}_{0.6}\text{Fe}_{0.4}\text{O}$), *Phys. Earth Planet. Inter.*, **129**, 301–311.
 Zhang, J., and D. J. Weidner (1999), Thermal equation of state of aluminium-enriched silicate perovskite, *Science*, **284**, 782–784.

J. D. Bass, Department of Geology, 245 Natural History Building, University of Illinois, 1301 W. Green Street, Urbana, IL 61801, USA.

H. Cardon and I. Daniel, Laboratoire de Sciences de la Terre, UMR 5570 CNRS–ENSL, Université Claude Bernard, Lyon, F-69622 Villeurbanne, France. (isabelle.daniel@univ-lyon1.fr)

G. Fiquet, Laboratoire de Minéralogie–Cristallographie UMR 7590, Université Paris VI, 140 rue Loumel, F-75015 Paris, France.

M. Hanfland, European Synchrotron Radiation Facility, BP 220, F-38043 Grenoble, France.

J. Zhang, Los Alamos National Laboratory, P.O. Box 1663, Los Alamos, NM 87545, USA.